



White matter microstructural organisation of interhemispheric pathways predicts different stages of bimanual coordination learning in young and older adults

Hamed Zivari Adab,¹ Sima Chalavi,¹ Iseult A. M. Beets,^{1,2} Jolien Gooijers,¹ Inge Leunissen,¹  Boris Cheval,^{3,4} Quinten Collier,⁵ Jan Sijbers,⁵ Ben Jeurissen,⁵ Stephan P. Swinnen¹ and Matthieu P. Boisgontier^{1,6} 

¹Movement Control and Neuroplasticity Research Group, Department of Movement Sciences, KU Leuven, Tervuurse Vest 101, Leuven, Belgium

²BrainCTR, Lilid bvba, Diest, Belgium

³Department of General Internal Medicine, Rehabilitation and Geriatrics, University of Geneva, Geneva, Switzerland

⁴Swiss NCCR "LIVES – Overcoming Vulnerability: Life Course Perspectives", University of Geneva, Geneva, Switzerland

⁵iMinds Vision Lab, University of Antwerp, Antwerp, Belgium

⁶Brain Behavior Laboratory, University of British Columbia, Vancouver, BC, Canada

Keywords: ageing, constrained spherical deconvolution-based tractography, diffusion-weighted imaging, motor learning, white matter transcallosal pathways

Abstract

The ability to learn new motor skills is crucial for activities of daily living, especially in older adults. Previous work in younger adults has indicated fast and slow stages for motor learning that were associated with changes in functional interactions within and between brain hemispheres. However, the impact of the structural scaffolds of these functional interactions on different stages of motor learning remains elusive. Using diffusion-weighted imaging and probabilistic constrained spherical deconvolution-based tractography, we reconstructed transcallosal white matter pathways between the left and right primary motor cortices (M1–M1), left dorsal premotor cortex and right primary motor cortex (LPMd–RM1) and right dorsal premotor cortex and left primary motor cortex (RPMd–LM1) in younger and older adults trained in a set of bimanual coordination tasks. We used fractional anisotropy (FA) to assess microstructural organisation of the reconstructed white matter pathways. Older adults showed lower behavioural performance than younger adults and improved their performance more in the fast but less in the slow stage of learning. Linear mixed models predicted that individuals with higher FA of M1–M1 pathways improve more in the fast but less in the slow stage of bimanual learning. Individuals with higher FA of RPMd–LM1 improve more in the slow but less in the fast stage of bimanual learning. These predictions did not differ significantly between younger and older adults suggesting that, in both younger and older adults, the M1–M1 and RPMd–LM1 pathways are important for the fast and slow stage of bimanual learning, respectively.

Introduction

With dedicated practice, our ability to perform complex motor skills (e.g. typing on a touch screen mobile) significantly improves. This ability to learn new motor and other skills is crucial at all ages and particularly in older adults (OA). It enables OA to counteract the adverse effects of ageing on sensorimotor control and to maintain functional independence (Swinnen *et al.*, 1998; Seidler *et al.*, 2010).

Behavioural studies have demonstrated that motor learning generally follows two distinct stages: (1) the early, fast learning stage in which improvement in performance is seen within the first training session and (2) the late, slow learning stage in which smaller gains are obtained across subsequent training sessions distributed over a single day, several days or weeks/months (Brashers-Krug *et al.*, 1996; Karni *et al.*, 1998; Doyon *et al.*, 2003). Depending on the task requirements, OA are often able to achieve considerable performance gains with training, similar to younger adults (YA) (Voelcker-Rehage & Willimczik, 2006; King *et al.*, 2013; Maes *et al.*, 2017). However, the question that has remained largely unanswered is the extent to which age modulates behavioural improvements in the fast and slow stages of motor learning.

In addition to learning-related behavioural aspects, functional brain studies have shown the involvement of cerebellar, subcortical

Correspondence: Hamed Zivari Adab, as above. E-mail: hamed.zivariadab@kuleuven.be

Received 17 October 2017, revised 22 December 2017, accepted 17 January 2018

Edited by Ali Mazaheri. Reviewed by Daniel Goble, Oakland University, USA; and William Staines, University of Waterloo, Canada

All peer review communications can be found with the online version of the article.

and cortical (including primary motor (M1), premotor (PM), prefrontal and parietal) structures in motor learning (Jueptner *et al.*, 1997; Doyon *et al.*, 2003; Debaere *et al.*, 2004; Floyer-Lea & Matthews, 2005; Puttemans *et al.*, 2005; Remy *et al.*, 2008; Hardwick *et al.*, 2013; Beets *et al.*, 2015). Aside from cortico-subcortical and cortico-cerebellar circuits involved in different stages of motor learning (Doyon *et al.*, 2003; Dayan & Cohen, 2011), transcallosal cortico-cortical functional interactions within the motor network may also play a relevant role (Kantak *et al.*, 2012). In this regard, previous work reported modulation of interhemispheric coupling between bilateral M1s and between dorsal PM and M1 (PMd–M1) during the fast bimanual learning stage (Andres *et al.*, 1999; Serrien & Brown, 2003; Sun *et al.*, 2007). Whether these results at the level of brain function extend to brain structure, and particularly white matter (WM) microstructural organisation, in YA and OA requires further investigation.

The WM microstructural organisation of the underlying network pathways is critical for the transfer of neuronal information through the network (Fields, 2008). This can be inferred *in vivo* using diffusion-weighted imaging (DWI). Previous DWI studies in YA have indicated associations between motor learning ability and the WM microstructural organisation of the corpus callosum (CC: containing fibres connecting the two hemispheres) (Sisti *et al.*, 2012), superior cerebellar peduncle (containing fibres connecting the cerebellum with motor and premotor areas) (Della-Maggiore *et al.*, 2009), PM cortex and cerebellum (Tomassini *et al.*, 2011). Of note, except for the study of Sisti *et al.* (2012), who investigated the slow stage of bimanual learning, the other two studies focused on the fast stage of unimanual motor learning. Two unimanual motor learning DWI studies included both OA and YA groups. Bennett *et al.* (2011) showed an association between the microstructural organisation of the WM pathway connecting caudate nucleus to dorsolateral prefrontal cortex and the fast and slow stages of unimanual motor learning in both OA and YA. More recently, Schulz *et al.* (2014) found correlations between the WM microstructural organisation of several cortico-cortical pathways connecting M1 to premotor areas (including PMd) and the slow stage of unimanual motor learning which were present only in OA.

In sum, the extent to which WM microstructural organisation predicts different stages of bimanual coordination learning, particularly in OA, is still unclear. Moving both hands in an organised manner in both space and time is required in many activities of daily living, which support functional independence. Bimanual movements occur twice as often as unimanual movements during activities of daily living (Vega-Gonzalez & Granat, 2005). Furthermore, bimanual (re-) training is frequently discussed in the context of neurorehabilitation in stroke patients (Reinkensmeyer *et al.*, 2016; Kantak *et al.*, 2017). These indications provide a strong impetus for exploring the neural basis of bimanual motor learning in OA.

Here, we investigated the extent to which (1) ageing impacts the fast and slow stages of bimanual motor learning, (2) WM microstructural organisation of transcallosal pathways involving M1 and PMd predicts bimanual motor learning and (3) whether the latter prediction is affected by age. We hypothesised that bimanual coordination performance improves in both stages of learning for both YA and OA (Maes *et al.*, 2017) and that these learning effects are age-dependent, with lower learning rates in OA. Recent studies revealed that WM microstructural organisation of left PMd–right M1 (LPMd–RM1) and M1–M1 pathways predict bimanual performance in OA (Serbruyns *et al.*, 2015; Fujiyama *et al.*, 2016a,b). However, RPMd also appeared to be particularly involved in performing complex bimanual tasks (Sadato *et al.*, 1997; Wenderoth *et al.*, 2004;

Aramaki *et al.*, 2006; Van den Berg *et al.*, 2010). Accordingly, we hypothesised that the WM microstructural organisation of the pathways linking M1–M1 and PMd–M1 would predict bimanual motor learning performance. Because previous structural imaging studies have demonstrated age-dependent WM microstructural alterations of the brain (Sullivan & Pfefferbaum, 2006; Giorgio *et al.*, 2010) predicting age-dependent differences in motor tasks performance (Zahr *et al.*, 2009; Sullivan *et al.*, 2010; Voineskos *et al.*, 2012), we hypothesised that age may also modulate the effect of WM microstructural organisation on bimanual motor learning.

Materials and methods

Participants

Twenty-six YA and 25 OA (right-handed; Oldfield, 1971) volunteers participated in the study. Three OA were excluded due to brain lesions and/or extreme atrophy as identified by a trained neuroradiologist. In addition, four YA were excluded: one due to poor DWI quality and presence of artefacts, two due to excessive head movements during DWI acquisition and one dropout. As a result, 22 OA (age: 68.41 ± 5.58 years; 12 females) and 22 YA (age: 21.05 ± 2.48 years; 13 females) were included in the analyses. The groups did not differ significantly with respect to gender ($\chi^2(1) = 0.09$, $P = 0.76$). All participants had normal or corrected-to-normal vision, and none reported neurological, psychiatric or cardiovascular disorders. This study was carried out in accordance with the Declaration of Helsinki (1964) and was approved by the Medical Ethics Committee UZ KU Leuven, Belgium. Participants were financially compensated for participation and provided written informed consent prior to the experiment.

Bimanual tracking task

We used a bimanual tracking task in which two dials controlled the direction and speed of a cursor on a computer screen: the right dial controlled displacement along the x-axis and the left dial along the y-axis (Fig. 1A; for details see Sisti *et al.*, 2011; Gooijers *et al.*, 2013; Beets *et al.*, 2015; Chalavi *et al.*, 2016). During each 9-s trial of the task, a white target dot moved over a blue line at a constant speed from start (centre of the screen) to end (Fig. 1B). The participant was instructed to track the target dot as closely as possible by rotating both dials simultaneously. Four coordination patterns imposed by the line direction were tested: both hands rotating inwards, outwards, clockwise or counterclockwise. Each pattern was performed with five distinct interhand frequency ratios, comprising 1 : 1, 1 : 2, 1 : 3, 2 : 1 and 3 : 1 (left hand: right hand). Thus, the combination of coordination patterns and frequency ratios resulted in 20 task variations, each being represented by a distinct target line (Fig. 1C). The intertrial interval was 3 s.

Experimental set-up and procedure

This study was part of a larger multimodal structural and fMRI project investigating the neural mechanisms underlying bimanual task performance (Beets *et al.*, 2015) and consisted of seven training sessions spread across 14 calendar days. On the first and seventh training session, hereafter referred to as Pre and Post, respectively, participants were trained with the bimanual tracking task in the MRI scanner while lying in a supine position (Fig. 1A), elbows flexed at 45° and forearms resting on pillows. Excessive head movements were prevented by a bite-bar and foam cushions. Visual stimuli were

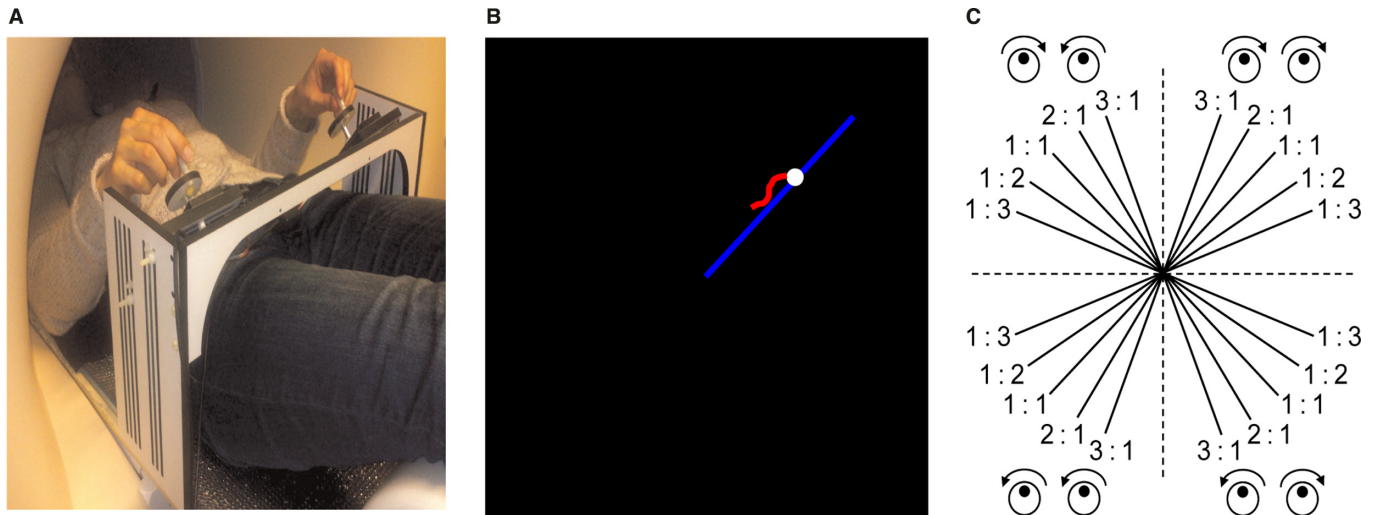


FIG. 1. Experimental set-up (A) in the scanner on training sessions 1 (Pre) and 7 (Post). (B) A typical feedback trial in which the subject had to track the white target dot moving along the blue target line for 9 s by simultaneous clockwise rotation of the left and right-hand dials with the same speed (1 : 1 ratio). Concurrent visual feedback representing the actual target error was shown in red. The red curve was absent for the no-feedback trials on training sessions Pre and Post and was given 1 s after the trial on training sessions 2–6. (C) Schematic drawing of the 20 target line directions corresponding to four different bimanual patterns and five possible frequency ratios.

projected by an LCD projector (Barco 6300, 1280×1024 pixels) onto a double mirror placed in front of the participant's eyes. A non-ferromagnetic apparatus with two dials (diameter = 5 cm) was placed over the participant's thighs. The participants were required to turn the handle of the dials with the fingers/wrist according to specific coordination patterns. Angular displacements were registered by means of non-ferromagnetic optical shaft encoders (HP, 2048 pulses per revolution, sampling frequency 100 Hz) fixed to the rotation axes of the dials. Version 8.5 of Laboratory Virtual Instrumentation Engineering Workbench (National Instruments) was used for task presentation and recording of the behavioural data.

On the Pre and Post scanning sessions, 96 task trials, divided into 48 trials with concurrent feedback (FB) and 48 trials without feedback (NFB), were performed. The concurrent FB was provided by means of a red cursor displaying the actual tracking trajectory based on the contribution of both limbs. The trials were spread over six fMRI/behavioural runs with inter-run interval of approximately 3 min (total session time: ~30 min). The order of trials was identical across participants in both Pre and Post sessions. The frequency ratio was pseudo-randomised across the FB and NFB conditions such that one-third of the trials was performed according to a 1 : 1 ratio, one-third according to a 1 : 2/2 : 1 ratio and one-third according to a 1 : 3/3 : 1 ratio. On the remaining five intermediate training sessions (sessions 2–6), participants were trained with the bimanual tracking task while seated in front of a computer screen (distance ~0.5 m) and with vision of the hands being occluded. On each of these training sessions, 10 blocks of 20 fully randomised trials were performed for ~1 h. The visual FB was displayed as in Pre and Post sessions in 50% of the trials. However, for the remaining 50% NFB trials, the entire actually produced trajectory was shown in red, concurrently with the required blue target line for a duration of 1 s after the trial. This was done to reduce the dependency on online visual FB and enhance learning in the NFB condition. In this study, all individual trials in the training session Pre (96 trials) were used to investigate the fast, early stage of learning, and all individual trials in the training sessions Pre and Post (96 trials each) were used to investigate the slow, late stage of learning. The behavioural results regarding training sessions 2–6 were published elsewhere (Beets *et al.*, 2015; Chalavi *et al.*, 2016).

Kinematic data analysis

MATLAB R2011b was used for the offline analyses of the behavioural data. On each trial, the positions (x , y) of the white target dot and the cursor were sampled at 100 Hz. For each trial, the Euclidian distance between the white target dot and the cursor position at each time point was calculated (900 distances in arbitrary units (a.u.)). Subsequently, the 'trial error score' was calculated by taking the average of these distances and was used as an indicator of accuracy with higher values reflecting lower bimanual performance.

Image acquisition

A Siemens 3-T Magnetom Trio MRI scanner (Siemens, Erlangen, Germany) with a 12-channel head coil was used for acquisition of brain images. For anatomical detail, a high-resolution whole brain T1-weighted structural image was obtained using magnetisation-prepared rapid gradient echo (MPRAGE; repetition time (TR)/echo time (TE) = 2300/2.98 ms, voxel size = $1 \times 1 \times 1.1$ mm³, field of view (FOV) = 240×256 mm², slices = 160 and flip angle = 9°). Then, a field map image was acquired using a dual gradient echo acquisition (GRE; TR = 1000 ms, TE2/TE1 = 5.69/3.23 ms, voxel size = $3 \times 3 \times 2.8$ mm³, matrix size = 64×64 , slices = 50; flip angle = 60°). DWIs were acquired prior to the fMRI/behavioural runs in training session Pre using the following parameters: single-shot spin echo planar with spectral attenuated inversion recovery (SPAIR), TR/TE = 10700/82 ms, voxel size = $2.2 \times 2.2 \times 2.4$ mm³, matrix size = 96×96 , slices = 60, flip angle = 90°, diffusion weighting of $b = 1000$ mm²/s applied in 64 non-collinear directions and one non-diffusion-weighted image.

Image processing

For each subject, first, the DWIs were visually inspected in three orthogonal views using ExploreDTI (Leemans *et al.*, 2009; www.exploredti.com) to identify visible artefacts, such as large signal drop-outs and geometric distortions (Tournier *et al.*, 2011). Second, the DWIs were preprocessed using MRtrix3 (J-D Tournier, Brain

Research Institute, Melbourne, Australia; www.mrtrix.org) which incorporates tools from FSL (Oxford University, Oxford, UK; <https://fsl.fmrib.ox.ac.uk>) when necessary. The preprocessing steps included the correction of the DWIs for the following: eddy-current-induced distortions and head motion (Andersson & Sotiropoulos, 2016), susceptibility-induced distortions (Jezzard & Balaban, 1995), bias fields (Tustison *et al.*, 2010) and Gibbs ringing (Kellner *et al.*, 2016). Third, the diffusion tensor model was fitted to each voxel of the corrected DWIs with a robust iterative reweighted least squares estimator (Collier *et al.*, 2015) and the fractional anisotropy (FA) map was calculated. Fourth, the warp to the Montreal Neurological Institute (MNI) standard space was obtained by non-linearly registering the FA map to the FMRIB58_FA template using tract-based spatial statistics (TBSS; Smith *et al.*, 2006) algorithm in FSL. The inverse of this warp was also calculated to warp MNI masks to subject's native space. Fifth, the T1 image was rigidly registered to the corrected DWIs to account for subject motion between the DW and structural scans, using mutual information as a similarity measure. Proper registration was checked visually.

In this study, average FA within the pathway of interest was used as an indicator of WM microstructural organisation to predict learning ability. FA ranges between zero and one with higher values reflecting higher microstructural organisation for the underlying white matter pathway (Beaulieu, 2002). To delineate the pathways of interest and calculate the average FA, the following main steps were performed.

Region of interest (ROI) creation

Using FSL, the bilateral M1 (anterior to the central sulcus) and PMd ROIs of Human Motor Area Template (HMAT; Mayka *et al.*, 2006; <http://lrlab.org/>) were extracted in MNI space. The ROIs were subsequently transformed from MNI to subject's native space using the inverse warp obtained previously. Of note, HMAT has been created based on 126 functional imaging studies performed with motor tasks. To further refine these masks based on individual anatomy, similar methodology as in Schulz *et al.* (2014, 2015) was used. First, the registered T1 image of each subject was segmented into grey and white matter (GM and WM) masks using SPM12 toolbox (<http://www.fil.ion.ucl.ac.uk/spm/>). Second, the GM and WM masks were thresholded at 0.2, non-zero voxels were mean dilated, and the resulting masks were multiplied to create the GM/WM border mask. Third, the GM/WM border mask and each M1 and PMd functional mask were multiplied to obtain the common voxels of these masks. This procedure, thus, integrates both functional and anatomical criteria to better define the ROIs. For each subject, all steps of ROI creation were visually inspected to ensure proper implementation. To restrict tractography (see next section) to the fibre tracts passing only through the CC, the following masks were created for each subject: (1) the CC inclusion mask was created by manual segmentation of the CC in the mid-sagittal plane and ± 3 slices on each side; (2) the exclusion midline mask was created by drawing the midline in every coronal slice without overlapping with the CC inclusion mask.

Constrained spherical deconvolution (CSD) and probabilistic tractography

Application of CSD to streamline tractography has been shown to increase reliability of tractography throughout the brain (Jeurissen *et al.*, 2011). A compulsory step in CSD is the 'response function' (RF) calculation which was made using Tournier's algorithm (Tournier *et al.*, 2013). Subsequently, CSD (with the maximum harmonic

order of 8) was employed to estimate fibre orientation distribution function (fODF) in each brain voxel (Tournier *et al.*, 2007). Probabilistic streamline tractography between ROIs was performed on fODFs, using a second-order integration over fibre orientation distributions (iFOD2) (Tournier *et al.*, 2010) algorithm which treats the fODF as a probability density function from which to sample. The following parameters were used for the tracking algorithm employed in the subject's native space: number of bidirectional generated streamlines = 10^6 , step size = 1 mm, maximum angle between successive steps = 40° , minimum streamline length = 40 mm, maximum streamline length = 250 mm and fODF cut-off value for initiating and terminating streamlines = 0.1. A symmetric and precise tracking result between two ROIs (for example between bilateral M1s) was obtained by considering both ROIs as 'seed' and 'include' masks. To guide the tracking algorithm for more accurate reconstruction of transcallosal pathways, the CC inclusion and the exclusion midline mask were also considered. To prevent 'cross talk' between the seed areas, the ROIs not involved in the active tracking were used as exclusion masks (Schulz *et al.*, 2014). All previously mentioned procedure was performed in MRtrix3.

Population mask of transcallosal pathways of interest and average FA calculation

To create the population mask for each transcallosal pathway of interest (Fig. 2A), the following procedure was performed in MRtrix3. (1) The tracking result of each subject was warped to MNI space. (2) The tract density image (TDI) was created by calculating the total number of streamlines passing each voxel (Calamante *et al.*, 2010). (3) 0.1% of the total number of successful streamlines with an absolute minimum of 2 per voxel was chosen to threshold the TDI. This threshold was chosen because it eliminated spurious fibre tracts based on visual inspection. (4) Binarised masks were summed across YA and OA to create the population mask which was then thresholded to select only those voxels that were found at least in 68% ($N = 30$; comparable with Schulz *et al.*, 2014) of the subjects. (5) The thresholded population mask of each pathway of interest was then transformed to the subject's native space to calculate the mean FA value within the subject's mask. The mean FA values and the \log_{10} of target error scores were used in the Statistical analysis section.

Statistical analysis

The data set was built with nested (i.e. multiple observations within a single participant) and crossed (i.e. participants observed in multiple bimanual coordination conditions) measurements. Thus, data were analysed using linear mixed models with crossed random factors. Linear mixed models take into account the sampling variability of both participants and conditions, thereby preventing a substantial inflation of false positives (i.e. type 1 error), whereas traditional analyses of variance such as ANOVAs disregard this sampling variability (Boisgontier & Cheval, 2016). Moreover, treating both participants and conditions as random effects allows generalising the results not only to the population of participants, but also to the population of conditions as well (Barr *et al.*, 2013). Finally, linear mixed models prevent information loss due to averaging over observations, as the model accounts for all single trials.

In this study, participants ($N = 44$) and bimanual coordination patterns ($n = 20$) served as random factors in the linear mixed models. These models were built using the R language lmerTest package, version 2.0-30 (<http://www.r-project.org/>). Examination of the statistical assumptions required for linear mixed models revealed

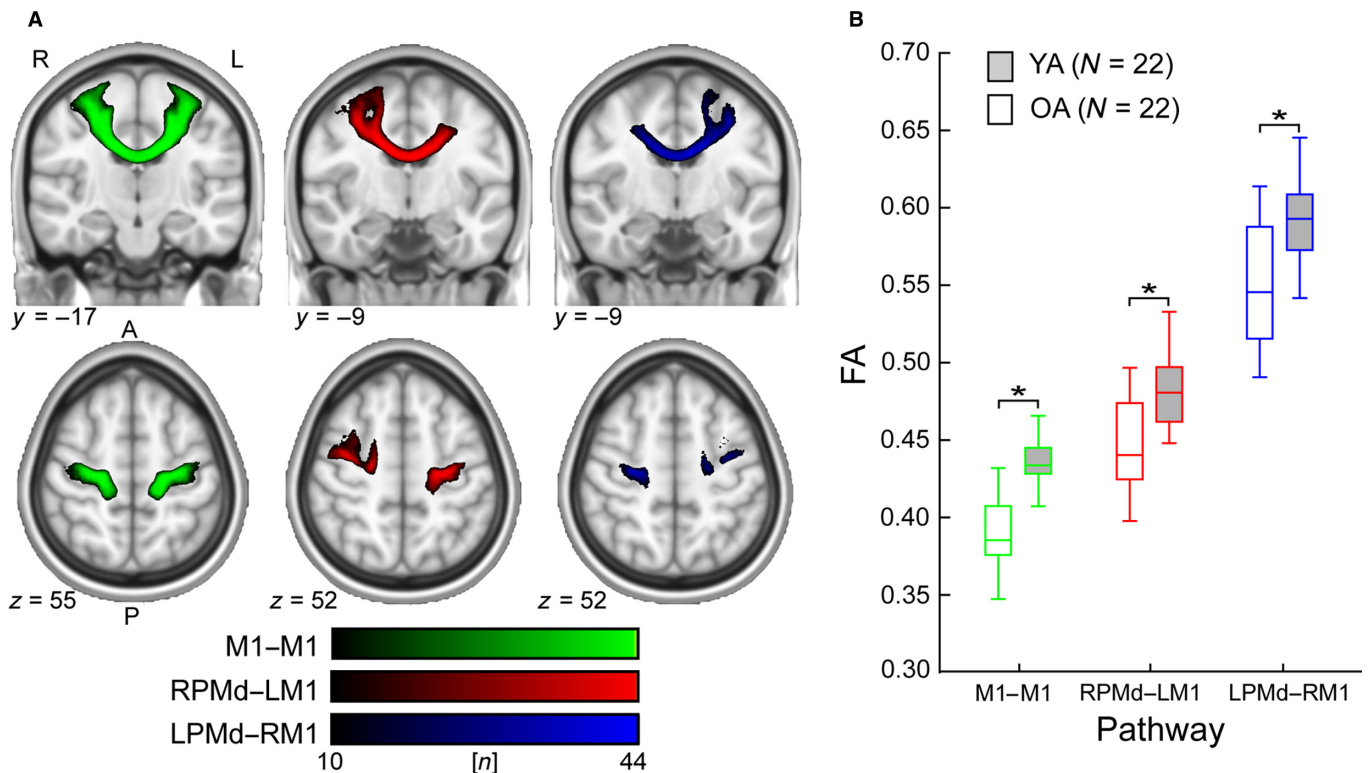


FIG. 2. Age-related differences in WM microstructural organisation of pathways of interest. (A) Representative sagittal (with y values) and axial (with z values) slices of population maps across YA and OA for M1-M1 (left panel), RPMd-LM1 (middle panel) and LPMd-RM1 (right panel) white matter pathways are overlaid on the MNI T1_{1mm} template. Colour bars indicate the number of subjects (n) showing overlap of the individual pathways. For visualisation purposes, images were thresholded to show only voxels common to at least 10 participants. (B) Mean FA of each pathway is shown for YA and OA. Middle bar: median; box: 1st and 3rd quartiles; whiskers: minimum and maximum. YA = young adults; OA = old adults; R = right; L = left; A = anterior; P = posterior; R/L PMd = right/left dorsal premotor cortex; L/R M1 = left/right primary motor cortex; fractional anisotropy = FA; N = number of subjects; * $P < 0.005$.

that residuals were not normally distributed and not centred on zero. Therefore, a \log_{10} transformation on target error score was conducted to normalise the distribution of residuals. Of note, for illustration purposes, the non-transformed data were plotted in the figures.

The first model of the series tested the effect of age on the fast (i.e. trial number 1–96 at Pre) (Table 1; Model 1) or slow (i.e. Pre vs. Post) learning stage (Table 2; Model 4) controlling for the effect of feedback. The second model of the series included the pathways' FA in interaction with the fast (Table 1; Model 2) or slow learning stage (Table 2; Model 5). The effect of the pathways' FA on the fast learning stage was assessed based on the interaction with trial number at Pre, and the effect on the slow learning stage was assessed based on the interaction with Pre vs. Post. Including trial as a predictor is only possible using linear mixed models, as traditional ANOVAs require averaging over trials. The third model of the series included a 3-way interaction term (pathways' FA \times learning stage (fast or slow) \times age) to investigate the extent to which the effect of FA on the fast (Table 1; Model 3) or slow (Table 2; Models 6a and b) learning stage was dependent on age. The continuous variables were centred on zero. Variance inflation factor (VIF; Belsley, 1991) was used to inspect signs of multicollinearity. Akaike information criterion (AIC; Sakamoto *et al.*, 1986) was used to assess the relative quality of statistical models. The best model of each series (fast and slow stage of learning) was selected based on the following: (1) multicollinearity, with models showing predictors with VIF scores higher than ten being discarded (Hair *et al.*, 1992) and (2) the fit of the models, with model with lower AIC score

indicating a more accurate fit for a given set of data (Sakamoto *et al.*, 1986).

Results

Age group differences in WM microstructural organisation

Figure 2A shows the population maps (across YA and OA) of transcallosal pathways connecting bilateral M1s, RPMd-LM1 and LPMd-RM1. In line with our expectation, significant age group differences were observed for all pathways of interest (separate Mann-Whitney U -tests, all P -values < 0.005), with higher FA in YA compared with OA (Fig. 2B).

Model selection

Model 1 (Table 1) investigating the effect of age on the fast learning stage showed an AIC score of 717.2. Model 2 (Table 1) testing the effect of pathways' FA on the fast stage of learning showed an AIC score of 682.5. Thus, Model 2 predicted the data more accurately than Model 1 ($\Delta AIC = -34.7$, negative ΔAIC means better fit). Model 3 (Table 1) investigating the age-dependent effect of pathways' FA on the fast stage of learning did not meet the assumptions on the multicollinearity with a VIF score of 20.8. Yet, a sensitive analysis testing each 3-way interaction of Model 3 individually confirmed that none was significant (all P -values > 0.254). Accordingly, Model 2 was the best model of the series testing the fast stage of learning.

TABLE 1. Predictors of fast stage of bimanual coordination learning. Log₁₀ target error scores (in a.u.) at Pre were used. Model 2 is the best model

| Fixed effects | Model 1 | | | Model 2 | | | Model 3 | | |
|------------------------------|-----------------------|----------------------|-------------------------|----------------|----------------------|-------------------------|----------------|------------------------|-------------------------|
| | b | SE | P | b | SE | P | b | SE | P |
| Intercept | 1.359 | 0.045 | < 2 × 10 ⁻¹⁶ | 1.308 | 0.055 | < 2 × 10 ⁻¹⁶ | 1.225 | 0.055 | < 2 × 10 ⁻¹⁶ |
| Feedback (vs. no feedback) | 0.168 | 0.008 | < 2 × 10 ⁻¹⁶ | 0.168 | 0.008 | < 2 × 10 ⁻¹⁶ | 0.168 | 0.008 | < 2 × 10 ⁻¹⁶ |
| FS learning (trials 1 to 96) | -0.002 | 3 × 10 ⁻⁴ | < 2 × 10 ⁻¹⁶ | -0.003 | 3 × 10 ⁻⁴ | < 2 × 10 ⁻¹⁶ | -0.003 | < 3 × 10 ⁻⁴ | < 2 × 10 ⁻¹⁶ |
| Age (OA vs. YA) | -0.384 | 0.056 | < 8 × 10 ⁻⁹ | -0.283 | 0.085 | 0.002 | -0.284 | 0.078 | < 8 × 10 ⁻⁴ |
| M1-MI | | | | -4.388 | 2.597 | 0.098 | -11.840 | 3.266 | < 8 × 10 ⁻⁴ |
| RPMd-LM1 | | | | 2.736 | 2.195 | 0.219 | 4.598 | 2.812 | 0.109 |
| LPMD-RM1 | | | | -0.125 | 1.248 | 0.920 | 2.742 | 1.549 | 0.084 |
| M1-MI × age | | | | | | | 14.210 | 4.637 | 0.004 |
| RPMd-LM1 × age | | | | | | | -3.502 | 3.855 | 0.369 |
| LPMD-RM1 × age | | | | | | | -5.027 | 2.229 | 0.029 |
| Age × FS learning | | | | | | | | | |
| M1-MI × FS learning | -2 × 10 ⁻⁴ | 3 × 10 ⁻⁴ | 0.435 | 0.002 | 5 × 10 ⁻⁴ | < 7 × 10 ⁻⁵ | 0.002 | < 5 × 10 ⁻⁴ | < 4 × 10 ⁻⁵ |
| RPMd-LM1 × FS learning | | | | -0.094 | 0.014 | < 4 × 10 ⁻¹¹ | -0.086 | 0.020 | < 3 × 10 ⁻⁵ |
| LPMD-RM1 × FS learning | | | | 0.055 | 0.012 | < 5 × 10 ⁻⁶ | 0.040 | 0.017 | 0.022 |
| M1-MI × FS learning × age | | | | 0.003 | 0.007 | 0.608 | 0.012 | 0.010 | 0.203 |
| RPMd-LM1 × FS learning × age | | | | | | | -0.021 | 0.029 | 0.476 |
| LPMD-RM1 × FS learning × age | | | | | | | 0.030 | 0.024 | 0.217 |
| | | | | | | | -0.020 | 0.014 | 0.154 |
| Random effects | σ ² | | | σ ² | | | σ ² | | |
| Participant | | | | | | | | | |
| Intercept | 0.031 | | | 0.029 | | | 0.022 | | |
| Condition | | | | | | | | | |
| Intercept | 0.009 | | | 0.009 | | | 0.009 | | |
| Residual | 0.065 | | | 0.065 | | | 0.065 | | |
| Highest VIF | 1.7 | | | 9.1 | | | 19.0 | | |
| AIC | | 717.2 | | | 682.5 | | | 679.8 | |

FS = fast stage of learning; OA = older adults; YA = younger adults; L = left; R = right; M1 = primary motor cortex; PMd = dorsal premotor cortex; AIC = Akaike information criterion; VIF = variance inflation factor; b = coefficient/estimate; SE = standard error; σ² = variance; *P < 0.05; **P < 0.01; ***P < 0.001. For more details about models see 'Statistical analysis' and 'Model selection'.

TABLE 2. Predictors of slow stage of bimanual coordination learning. Log₁₀ target error scores (in a.u.) at Pre and Post were used. Model 6b is the best model

| Fixed effects | Model 4 | | | | Model 5 | | | | Model 6a | | | | Model 6b | | | |
|------------------------------|----------------|----------------------|-------------------------|-----|----------------|----------------------|-------------------------|-----|----------------|----------------------|-------------------------|-----|----------------|----------------------|-------------------------|-----|
| | b | SE | P | | b | SE | P | | b | SE | P | | b | SE | P | |
| Intercept | 1.356 | 0.039 | < 2 × 10 ⁻¹⁶ | *** | 1.305 | 0.048 | < 2 × 10 ⁻¹⁶ | *** | 1.222 | 0.049 | < 2 × 10 ⁻¹⁶ | *** | 1.308 | 0.048 | < 2 × 10 ⁻¹⁶ | *** |
| Feedback (vs. no feedback) | 0.176 | 0.006 | < 2 × 10 ⁻¹⁶ | *** | 0.176 | 0.006 | < 2 × 10 ⁻¹⁶ | *** | 0.176 | 0.006 | < 2 × 10 ⁻¹⁶ | *** | 0.176 | 0.006 | < 2 × 10 ⁻¹⁶ | *** |
| FS learning (trials 1 to 96) | -0.002 | 1 × 10 ⁻⁴ | < 2 × 10 ⁻¹⁶ | *** | -0.002 | 1 × 10 ⁻⁴ | < 2 × 10 ⁻¹⁶ | *** | -0.002 | 1 × 10 ⁻⁴ | < 2 × 10 ⁻¹⁶ | *** | -0.002 | 1 × 10 ⁻⁴ | < 2 × 10 ⁻¹⁶ | *** |
| SS learning (Pre vs. Post) | -0.346 | 0.008 | < 2 × 10 ⁻¹⁶ | *** | -0.337 | 0.011 | < 2 × 10 ⁻¹⁶ | *** | -0.312 | 0.012 | < 2 × 10 ⁻¹⁶ | *** | -0.340 | 0.011 | < 2 × 10 ⁻¹⁶ | *** |
| Age (OA vs. YA) | -0.384 | 0.046 | < 2 × 10 ⁻¹⁰ | *** | -0.283 | 0.074 | < 4 × 10 ⁻⁴ | *** | -0.284 | 0.069 | < 2 × 10 ⁻⁴ | *** | -0.256 | 0.077 | 0.002 | ** |
| M1-M1 | | | | | -4.388 | 2.247 | 0.057 | | -11.840 | 2.878 | < 2 × 10 ⁻⁴ | *** | -4.956 | 2.286 | 0.035 | * |
| RPMd-LM1 | | | | | 2.735 | 1.899 | 0.157 | | 4.597 | 2.477 | 0.070 | | 2.938 | 1.897 | 0.129 | |
| LPMd-RM1 | | | | | -0.125 | 1.079 | 0.908 | | 2.743 | 1.365 | 0.050 | | 0.545 | 1.214 | 0.656 | |
| M1-M1 × age | | | | | | | | | 14.210 | 4.085 | 0.001 | ** | | | | |
| RPMd-LM1 × age | | | | | | | | | -3.501 | 3.396 | 0.308 | | | | | |
| LPMd-RM1 × age | | | | | | | | | -5.028 | 1.964 | 0.014 | * | -1.759 | 1.489 | 0.243 | |
| Age × SS learning | -0.047 | 0.012 | < 3 × 10 ⁻⁵ | *** | -0.065 | 0.018 | < 4 × 10 ⁻⁴ | *** | -0.079 | 0.019 | < 4 × 10 ⁻⁵ | *** | -0.088 | 0.019 | < 5 × 10 ⁻⁶ | *** |
| M1-M1 × SS learning | | | | | 2.922 | 0.559 | < 2 × 10 ⁻⁷ | *** | 5.016 | 0.803 | < 5 × 10 ⁻¹⁰ | *** | 3.416 | 0.571 | < 3 × 10 ⁻⁹ | *** |
| RPMd-LM1 × SS learning | | | | | -3.574 | 0.472 | < 5 × 10 ⁻¹⁴ | *** | -3.101 | 0.692 | < 8 × 10 ⁻⁶ | *** | -3.751 | 0.474 | < 3 × 10 ⁻¹⁵ | *** |
| LPMd-RM1 × SS learning | | | | | 0.564 | 0.268 | 0.036 | * | -1.194 | 0.381 | 0.002 | ** | -0.019 | 0.303 | 0.951 | |
| M1-M1 × SS learning × Age | | | | | | | | | -3.433 | 1.140 | 0.003 | ** | | | | |
| RPMd-LM1 × SS learning × Age | | | | | | | | | -1.075 | 0.948 | 0.257 | | | | | |
| LPMd-RM1 × SS learning × Age | | | | | | | | | 3.464 | 0.548 | < 3 × 10 ⁻¹⁰ | *** | 1.530 | 0.372 | < 4 × 10 ⁻⁵ | *** |
| Random effects | σ ² | | | | σ ² | | | | σ ² | | | | σ ² | | | |
| Participant | 0.023 | | | | 0.022 | | | | 0.017 | | | | 0.021 | | | |
| Intercept | | | | | | | | | | | | | | | | |
| Condition | | | | | | | | | | | | | | | | |
| Intercept | 0.009 | | | | 0.009 | | | | 0.009 | | | | 0.009 | | | |
| Residual | 0.067 | | | | 0.066 | | | | 0.066 | | | | 0.066 | | | |
| Highest VIF | 2.0 | | | | 9.3 | | | | 19.4 | | | | 9.7 | | | |
| AIC | 1379.4 | | | | 1325.6 | | | | 1280.3 | | | | 1312.2 | | | |

FS and SS = fast and slow stage of learning; OA = older adults; YA = younger adults; L = left; R = right; M1 = primary motor cortex; PMd = dorsal premotor cortex; AIC = Akaike information criterion; VIF = variance inflation factor; b = coefficient/estimate; SE = standard error; σ² = variance; *P < 0.05; **P < 0.01; ***P < 0.001. For more details about models see 'Statistical analysis' and 'Model selection'.

Model 4 (Table 2) investigating the effect of age on the slow stage of learning showed an AIC score of 1379.4. Model 5 (Table 2) testing the effect of pathways' FA on the slow learning stage predicted the data more accurately than Model 1 ($\Delta\text{AIC} = -53.8$). Model 6a (Table 2) investigating the age-dependent effect of pathways' FA on the slow stage of learning did not meet the assumptions on the multicollinearity with a VIF score of 19.4. However, sensitive analyses testing each 3-way interaction of Model 6a individually revealed that the 3-way interaction involving the LPMd-RM1 pathway was significant ($P < 9 \times 10^{-4}$) but not the ones involving M1-M1 ($P = 0.087$) and RPMd-LM1 ($P = 0.130$) pathways. Therefore, Model 6b (Table 2) was tested to include the 2-way interactions of Model 5 and the significant 3-way LPMd-RM1 FA \times slow-stage learning \times age interaction. This model met the multicollinearity assumption with a VIF score of 9.7 and predicted the data more accurately than Model 4 and Model 5 ($\Delta\text{AIC} = -67.2$ and -13.4 , respectively). Accordingly, Model 6b was the best model of the series testing the slow stage of learning.

Effects of age on the fast and slow stage of learning

Model 2 (Table 1) showed a significant fast-stage learning \times age interaction ($b = 0.002$; $P < 7 \times 10^{-5}$; Fig. 3A) indicating that the fast stage of learning significantly differs between YA and OA. This effect of age was independent of microstructural organisation of the WM pathways as they were included in this model. Simple slope analysis revealed that target error score decreased more from trial 1 to 96 in OA ($b = -0.003$; $P < 2 \times 10^{-16}$) than in YA ($b = -0.001$; $P < 3 \times 10^{-5}$). Simple effect analysis revealed that target error score was also lower in YA than OA at trial 1 ($b = 0.370$; $P < 2 \times 10^{-4}$) and to a smaller extent at trial 96 ($b = 0.284$; $P = 0.002$).

Model 6b (Table 2) showed a significant slow-stage learning (i.e. Pre vs. Post) \times age interaction ($b = -0.088$; $P < 5 \times 10^{-6}$; Fig. 3B) indicating that the slow stage of learning significantly differs between YA and OA. This effect of age was independent of microstructural organisation of the WM pathways as they were included in this model. Simple slope analysis revealed that target error score decreased more from Pre to Post in YA ($b = -0.428$; $P < 2 \times 10^{-16}$) than in OA ($b = -0.340$; $P < 2 \times 10^{-16}$). Simple effect analysis revealed that target error score was lower in YA than OA at Pre ($b = 0.256$; $P = 0.002$) and to a bigger extent at Post ($b = 0.344$; $P < 5 \times 10^{-5}$). Altogether, these results indicated that

performance gain was larger in OA compared with YA in the fast stage of bimanual learning. Conversely, the gain in performance was larger in YA compared with OA in the slow stage.

Effects of WM microstructural organisation on the fast stage of learning

Model 2 (Table 1) showed a significant fast-stage learning (i.e. trials 1–96 at Pre) \times M1–M1 FA interaction ($b = -0.094$; $P < 4 \times 10^{-11}$; Fig. 4A), indicating that the effect of fast-stage learning significantly varies depending on the level of M1–M1 FA. Simple slope analysis revealed that target error score increased from trial 1 to 96 when M1–M1 FA was low (-1 standard deviation) ($b = 0.002$; $P = 0.009$) and decreased when FA was high ($+1$ standard deviation) ($b = -0.004$; $P < 2 \times 10^{-16}$). Simple effect analysis revealed that target error score did not significantly differ between low and high M1–M1 FA at trial 1 ($b = 0.050$; $P = 0.985$), but was lower at trial 96 for high compared with low M1–M1 FA values ($b = -8.826$; $P = 0.002$). In this model, a significant fast-stage learning \times RPMd–LM1 FA interaction ($b = 0.055$; $P < 5 \times 10^{-6}$; Fig. 4B) also indicated that the fast-stage learning slopes were dependent on RPMd–LM1 FA. Simple slope analysis revealed that target error score decreased from trial 1 to 96 when RPMd–LM1 FA was low ($b = -0.003$; $P < 6 \times 10^{-12}$), but not when it was high ($b = 6 \times 10^{-4}$; $P = 0.263$). Simple effect analysis revealed that target error score did not significantly differ between low and high RPMd–LM1 FA at trial 1 ($b = 0.050$; $P = 0.985$), but was lower at trial 96 for low compared with high RPMd–LM1 FA ($b = 5.342$; $P = 0.022$). Model 2 also showed a non-significant fast-stage learning \times LPMd–RM1 FA interaction ($b = 0.003$; $P = 0.608$) indicating that fast-stage learning slopes were not dependent on LPMd–RM1 FA. In sum, the model predicted higher absolute performance gain in the fast stage of bimanual learning when M1–M1 FA is high or when RPMd–LM1 FA is low, irrespective of age. Furthermore, LPMd–RM1 FA did not affect absolute performance gain in the fast stage of bimanual learning.

Effects of WM microstructural organisation on the slow stage of learning

Model 6b (Table 2) showed a slow-stage learning (i.e. Pre vs. Post) \times M1–M1 FA interaction ($b = 3.416$; $P < 3 \times 10^{-9}$; Fig. 5A), which indicated that slow-stage learning slopes were dependent on M1–M1 FA. Simple slope analysis revealed that target error score decreased from Pre to Post when M1–M1 FA was low ($b = -0.531$;

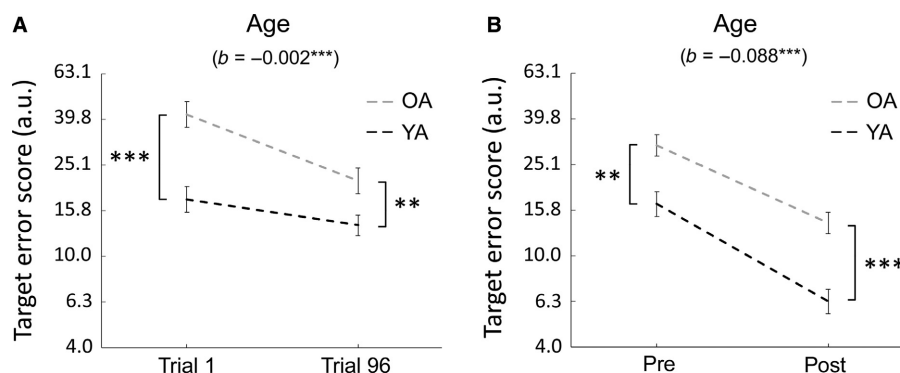


FIG. 3. Age as predictor of the (A) fast (trial 1 to 96 of Pre) and (B) slow stage (Pre vs. Post) of bimanual coordination learning. Mean (\pm standard error) is shown. YA = young adults; OA = old adults; a.u. = arbitrary units; b = coefficient/estimate; $**P < 0.01$; $***P < 0.001$.

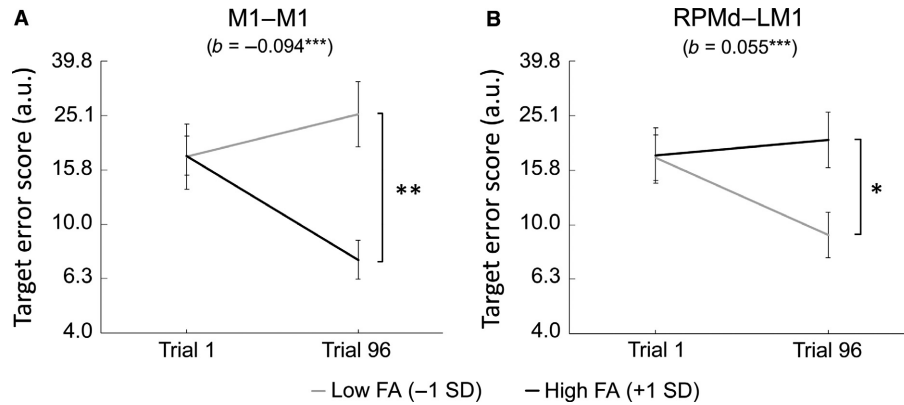


FIG. 4. White matter pathways predicting the fast stage (trial 1 to 96 of Pre) of bimanual coordination learning across YA and OA: (A) M1–M1 FA and (B) RPMd–LM1 FA. Mean (\pm standard error) is shown. YA = young adults; OA = old adults; a.u. = arbitrary units; FA = fractional anisotropy; RPMd = right dorsal premotor cortex; LM1 = left primary motor cortex; SD = standard deviation; b = coefficient/estimate; * P < 0.05; ** P < 0.01; *** P < 0.001.

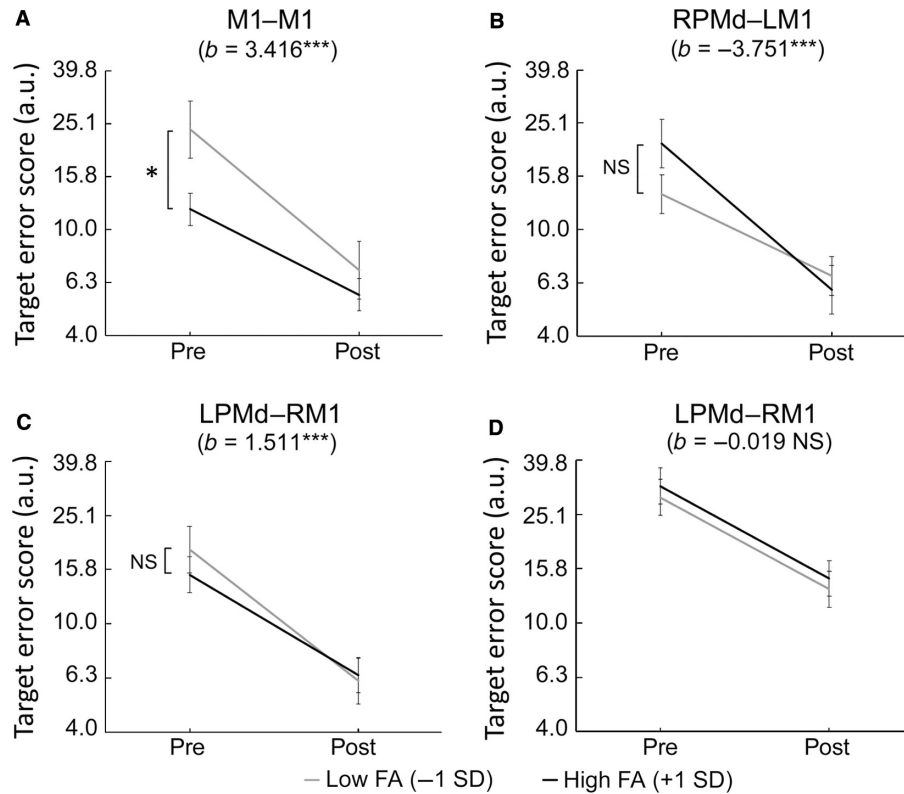


FIG. 5. White matter pathways predicting the slow stage (Pre vs. Post) of bimanual coordination learning: (A) M1–M1 FA and (B) RPMd–LM1 FA across YA and OA. Because of a significant 3-way interaction of LPMd–RM1 FA \times slow-stage learning \times age for this predictor, the results are shown for (C) YA and (D) OA, separately. Mean (\pm standard error) is shown. YA = young adults; OA = old adults; a.u. = arbitrary units; FA = fractional anisotropy; R/L PMd = right/left dorsal premotor cortex; L/R M1 = left/right primary motor cortex; SD = standard deviation; b = coefficient/estimate; NS = not significant, P > 0.05; * P < 0.05; *** P < 0.001.

$P < 2 \times 10^{-16}$) and to a smaller extent when FA was high ($b = -0.324$; $P < 2 \times 10^{-16}$). Simple effect analysis revealed that target error score was higher in low vs. high M1–M1 FA at Pre ($b = -4.956$; $P = 0.035$), but not at Post ($b = -1.541$; $P = 0.504$). In this model, a significant slow-stage learning \times RPMd–LM1 interaction indicated that slow-stage learning slopes were dependent on RPMd–LM1 FA ($b = -3.751$; $P < 3 \times 10^{-15}$; Fig. 5B). Simple slope analysis revealed that target error score decreased from Pre to Post when RPMd–LM1 FA was low ($b = -0.306$; $P < 2 \times 10^{-16}$) and to a

bigger extent when FA was high ($b = -0.550$; $P < 2 \times 10^{-16}$). However, simple effect analysis revealed that target error score did not significantly differ between low and high RPMd–LM1 FA at Pre ($b = 2.938$; $P = 0.129$) and Post ($b = -0.813$; $P = 0.670$). Model 6b also showed a 3-way slow-stage learning \times LPMd–RM1 \times age interaction ($b = 1.530$; $P < 4 \times 10^{-5}$) with a 2-way significant slow-stage learning \times LPMd–RM1 interaction in YA (Fig. 5C; $b = 1.511$; $P < 2 \times 10^{-5}$) but not in OA (Fig. 5D; $b = -0.019$; $P = 0.951$). In YA, simple slope analysis revealed that target error score decreased

from Pre to Post when LPMd–RM1 FA was low ($b = -0.485$; $P < 2 \times 10^{-16}$) and to a smaller extent when it was high ($b = -0.373$; $P < 2 \times 10^{-16}$). By contrast, in OA, target error score decreased from Pre to Post to the same extent for low ($b = -0.339$; $P < 2 \times 10^{-16}$) and high ($b = -0.340$; $P < 2 \times 10^{-16}$) LPMd–RM1 FA. Simple effect analysis revealed that target error score did not significantly differ between low and high LPMd–RM1 FA at Pre (YA: $b = -1.214$, $P = 0.395$; OA: $b = 0.545$, $P = 0.656$) and Post (YA: $b = 0.297$, $P = 0.835$; OA: $b = 0.526$, $P = 0.667$) in YA and OA. In sum, the model predicted higher absolute performance gain in the slow stage of bimanual learning when RPMd–LM1 FA is high or when M1–M1 FA is low, irrespective of age. Furthermore, lower LPMd–RM1 FA in YA predicted bigger performance gain in the slow stage of bimanual learning.

Discussion

The present study investigated the extent to which (1) age determined the absolute performance gains in the fast and slow stages of bimanual learning, (2) WM microstructural organisation of the pathway between bilateral M1s and heterotopic pathways between M1 and PMd predicted bimanual motor learning in these stages and (3) the latter predictions were not affected by healthy ageing. DWI and CSD-based probabilistic tractography were used to delineate these transcallosal WM pathways in YA and OA. Behavioural results showed that both OA and YA improved their absolute performance in both fast and slow stages of bimanual learning. However, this improvement was larger during the fast (early) learning stage in OA and during the slow (later) stage in YA. The statistical models predicted that individuals with higher FA of M1–M1 and RPMd–LM1 WM pathways showed larger performance gain in the fast and slow stage of bimanual learning, respectively. These predictions were age-independent.

Fast and slow stages of learning in YA and OA

Our findings support previous results showing that bimanual performance is lower in OA than YA (Swinnen *et al.*, 1998; Voelcker-Rehage & Willimczik, 2006; Fling *et al.*, 2011; Serbruyns *et al.*, 2015). The lower performance level in OA is generally attributed to the age-related alterations in the central and peripheral nervous system as well as the neuromuscular system (Seidler *et al.*, 2010). In line with previous studies, both age groups showed motor performance improvement during both fast and slow stages of learning (Brashers-Krug *et al.*, 1996; Karni *et al.*, 1998; Doyon *et al.*, 2003). Furthermore, compared with YA, OA showed more gains in performance during the fast but less during the slow stage of bimanual learning. With respect to the fast learning stage, our results seem to be inconsistent with previous work showing higher (Swinnen *et al.*, 1998; Wishart *et al.*, 2002; Perrot & Bertsch, 2007; Cirillo *et al.*, 2010) or similar (Howard & Howard, 1992; Cirillo *et al.*, 2011; Berghuis *et al.*, 2016) absolute performance gain in YA as compared to OA during the first day of practice. However, consistent with our findings, Brown *et al.* (2009) showed superior capacity of OA over YA to acquire new motor skills in the first session of training. Importantly, our analysis controlled for the level of performance and thereby ruled out this potential confound. Therefore, our results clearly support the fact that the fast learning stage of motor learning is not affected by ageing. With respect to the slow learning stage, our results support previous work showing higher absolute performance gain in YA as compared to OA after 5 days of practice in a demanding bimanual coordination task (Ren *et al.*, 2015) or 4 days

of practice in a juggling task (Perrot & Bertsch, 2007). Our findings seem to be in contrast with other juggling (Voelcker-Rehage & Willimczik, 2006) and bimanual coordination (Pauwels *et al.*, 2015) studies indicating, respectively, equal or larger absolute performance gain in OA than YA after several days of practice. However, the results from these latter studies should be considered cautiously as they may be related to a larger window for improvement in OA due to lower initial performance levels.

In sum, our findings showed higher learning rates in OA during the early phase of learning, whereas learning rates were higher in YA during the late phase. This result could be related to previous studies showing that motor tasks learned more quickly are also the ones showing lower retention (Pauwels *et al.*, 2015). Although these previous results were obtained by manipulating task complexity, they may suggest that the learning process we observed here in YA could be more robust over time than the one in OA. This would support previous results showing that retention is higher in YA than in OA (Pauwels *et al.*, 2015). It is worth noting that the diversity of the bimanual tasks and the potential interactions of task-related factors (e.g. task complexity, task difficulty and the presence vs. absence of augmented feedback) and training-related factors (e.g. baseline performance and number of trials) with ageing effects may contribute to inconsistencies in the literature (Maes *et al.*, 2017). In the current study, all these factors were controlled in the models (augmented vs. no augmented feedback, trial number, baseline performance as fixed factors, condition complexity and difficulty as random factors), which makes our findings particularly relevant.

Microstructural organisation in OA

The spatial configuration of the homotopic transcallosal pathways between M1s was in good agreement with previous reports (Zarei *et al.*, 2006; Wahl *et al.*, 2007; Fling *et al.*, 2013; Schulz *et al.*, 2014). Regarding the heterotopic pathways between PMd and M1, anatomical data in animals have indicated the presence, although sparse, of such direct pathways (Marconi *et al.*, 2003). Using CSD-based probabilistic tractography, we delineated these pathways with a high consistency across subjects and confirmed recent imaging data in humans (Boorman *et al.*, 2007; Schulz *et al.*, 2014; Ruddy *et al.*, 2017). These human imaging data taken together with the animal anatomical data may further support the existence of such direct pathways in humans. We estimated the microstructural organisation of the underlying WM pathway of interest via FA. We found that, for all the reconstructed interhemispheric pathways of interest, the mean FA values were lower in OA than YA, which supports numerous studies indicating reductions in WM microstructural organisation with ageing (Nusbaum *et al.*, 2001; Sullivan & Pfefferbaum, 2006, 2007; Minati *et al.*, 2007; Giorgio *et al.*, 2010; Serbruyns *et al.*, 2015).

WM pathways, motor learning and ageing

Previous work has indicated the dynamic modulation of activity in a widely distributed network of neocortical structures including, but not limited to, M1 and PMd during the fast and slow stages of bimanual learning (Debaere *et al.*, 2004; Puttemans *et al.*, 2005; Remy *et al.*, 2008; Ronsse *et al.*, 2011; Beets *et al.*, 2015). In addition to intraregional modulation of activity, the alteration of inter-regional functional connectivity also plays an important role in bimanual learning (Andres *et al.*, 1999; Serrien & Brown, 2003; Sun *et al.*, 2007; Heitger *et al.*, 2012). However, functional

interactions between brain regions may also be contingent upon the structure of the underlying WM pathways (Fields, 2008).

WM pathways predicting performance in the fast and slow stages of motor learning

Studies using functional connectivity showed that changes in the coupling of M1–M1 activity occur during the fast stage of bimanual learning (Andres *et al.*, 1999; Serrien & Brown, 2003; Sun *et al.*, 2007). Thus, our results showing that individuals with higher FA in the M1–M1 WM pathway improved more than individuals with lower FA in the fast learning stage support these functional studies and provide a structural foundation for the functional interactions during the fast stage of bimanual learning. Previous work has indicated the role of PMd in premovement cognitive processes such as action selection and planning (Hoshi & Tanji, 2002, 2004; O'Shea *et al.*, 2007), which are important elements for learning of the visuomotor task used in the current study. The PMd is functionally lateralised, such that the LPMd is activated during performance of simple unimanual and bimanual movements, whereas the RPMd is particularly active during complex bimanual movements (Van den Berg *et al.*, 2010). The involvement of PMd in motor learning is also lateralised towards the LPMd during the early stage of learning (for review see Schubotz & Von Cramon, 2003). However, the models from our analyses suggested no effect of LPMd–RM1 FA and an adverse impact of higher RPMd–LM1 FA on the fast stage of learning. In other words, higher FA between RPMd and LM1 may suggest that this pathway interferes with the fast learning stage. The absence of effect of the LPMd–RM1 pathway is not in line with previous functional activation findings showing consistent brain activity of LPMd in learning of unimanual motor tasks (Hardwick *et al.*, 2013). This discrepancy suggests that including the less accurate non-dominant limb in the integrated bimanual control structure modifies the predictive value of right and left PMd-related metrics in motor learning.

Our results showed that individuals with lower FA in the M1–M1 WM pathway improved more than individuals with higher FA in the slow learning stage. This result was mainly explained by a difference at Pre but not at Post training session, which suggested that the M1–M1 pathway became less important for the performance in the advanced learning stage. The models also suggested a beneficial impact of higher RPMd–LM1 FA on the slow stage of learning. In other words, higher FA between RPMd and LM1 increased the performance gain in the slow learning stage, suggesting that this communication should be maximised at this stage. This result supports previous work showing the involvement of RPMd during advanced stages of learning and in memory storage (for review see Schubotz & Von Cramon, 2003). However, this result should be cautiously considered as this interaction did not result in significant differences in performance at Pre and Post training sessions between individuals with lower and higher RPMd–LM1 FA.

Based on these findings, and tentatively assuming that an enhanced microstructural organisation of white matter connections between two brain areas may benefit interaction between these areas, we could speculate that the fast stage of learning benefits from strong interactions between brain areas involved in movement execution (M1–M1) to develop the basic temporal organisation of the bimanual movement structure. Further refinement of performance is observed during the slow stage of learning. While we consider left PMd an important brain area to plan and control bimanual movements (Fujiyama *et al.*, 2016a,b), the non-dominant limb is the weaker part in the bimanual chain. Therefore, the (direct and/or

indirect) input from right PMd to left M1 is likely critical for performance refinement.

Age does not influence the effect of WM microstructural organisation on learning

A recent study by Schulz *et al.* (2014) showed associations between the slow stage of unimanual sequence learning and FA of WM pathways connecting sensorimotor cortical areas, but only in OA. The authors indicated that the lack of associations in YA could be due to the small sample size preventing sufficient statistical power. In the current study, instead of averaging performance across trials which limits the statistical power, we made use of single trials in the linear mixed models. Contrary to Schulz *et al.* (2014), we reported similar effects for both YA and OA regarding the role of M1–M1 and RPMd–LM1 WM microstructural organisation in learning. The lack of a significant interaction with age in these pathways is consistent with previous work indicating a link between FA of the WM pathway connecting dorsolateral prefrontal cortex and caudate nucleus during the slow stage of unimanual learning in both YA and OA (Bennett *et al.*, 2011). In our study, we did show an interaction between LPMd–RM1 FA \times slow learning stage \times age with low LPMd–RM1 FA predicting higher learning rates than high FA in YA. The result suggested an adverse impact of higher LPMd–RM1 FA on the slow stage of learning in YA but not in OA. However, these results in YA should be cautiously considered as performance between individuals with lower and higher LPMd–RM1 FA did not significantly differ at Pre and Post training sessions.

Conclusion

Our results showed that (1) age determines the learning gains in the fast and slow learning stages with larger absolute performance improvement in OA during the fast stage and in YA during the slow learning stage, (2) higher FA of the M1–M1 WM pathway predicts larger performance gain in the fast stage of bimanual learning, whereas higher FA of the RPMd–LM1 WM pathway predicts higher gain in the slow stage, and (3) age does not affect the latter predictions. These results suggest that, in both YA and OA, the M1–M1 and RPMd–LM1 WM pathways are important for the fast and slow stage of bimanual learning, respectively.

Among the strengths of the present study is the use of CSD-based probabilistic tractography which is more reliable in tracking within regions including crossing fibres compared to other multifibre methods (Wilkins *et al.*, 2015). However, we note that the acquisition of recently developed multishell DWI could enhance the tracking even more (Jeurissen *et al.*, 2014). Another strength is the use of a statistical approach (i.e. linear mixed models) that limits false-positive rates. Because brain stimulation might alleviate impaired skill acquisition particularly in OA (Zimmerman *et al.*, 2013), additional knowledge of age-related structural alterations and their specific associations with motor functions will pave the way for optimising brain stimulation that is propagated via these structural pathways.

Acknowledgements

We thank all participants taking part in this study, René Clerckx for programming of the behavioural task and Dan Orsholits for his help with data analysis. This work was supported by the Research Foundation—Flanders (FWO) (G089818N), and FWO Excellence of Science funding (EOS 30446199), KU Leuven Research Fund (C16/15/070), an FWO post-doctoral fellowship and research grant (1504015N) to MPB and a post-doctoral mandate internal grant by KU Leuven (PDM/16/168) to HZA.

Conflict of interest

We have no conflict of interest or competing interests to disclose.

Author contributions

HZA, IAMB, MBP and SPS designed the study. IAMB and JG performed the experiment. HZA, SC, IL, QC, JS and BJ contributed in image processing and analysis. MPB and BC performed statistical analyses. HZA and MBP wrote the first draft of the manuscript, but all authors contributed in revising the work and approved the final version of the manuscript.

Data accessibility

The anonymised raw data are freely available on the Open Science Framework: Zivari, A.H., Chalavi, S., Beets, I.A., Gooijers, J., Leunissen, I., Cheval, B., Collier, Q., Sijbers, J., Jeurissen, B., Swinnen, S.P. and Boisgontier, M.P. (2017) White matter microstructural organisation of interhemispheric pathways predicts different stages of bimanual coordination learning in young and older adults. <https://osf.io/wcfbd>.

Abbreviations

AIC, Akaike information criterion; b, coefficient/estimate; CC, corpus callosum; CSD, constrained spherical deconvolution; DWI, diffusion-weighted imaging; FA, fractional anisotropy; fMRI, functional magnetic resonance imaging; FOV, field of view; FS, fast stage; GM, grey matter; GRE, gradient echo; HMT, human motor area template; L, left; M1, primary motor cortex; MNI, Montreal Neurological Institute; MPRAGE, magnetisation-prepared rapid gradient echo; OA, older adults; ODF, orientation distribution function; PMD, dorsal premotor cortex; ROI, region of interest; R, right; SD, standard deviation; SE, standard error; SPAIR, spectral attenuated inversion recovery; SS, slow stage; TE, echo time; TR, repetition time; VIF, variance inflation factor; WM, white matter; YA, young adults.

References

- Andersson, J.L.R. & Sotiropoulos, S.N. (2016) An integrated approach to correction for off-resonance effects and subject movement in diffusion MR imaging. *NeuroImage*, **125**, 1063–1078.
- Andres, F.G., Mima, T., Schulman, A.E., Dichgans, J., Hallett, M. & Gerloff, C. (1999) Functional coupling of human cortical sensorimotor areas during bimanual skill acquisition. *Brain*, **122**, 855–870.
- Aramaki, Y., Honda, M., Okada, T. & Sadato, N. (2006) Neural correlates of the spontaneous phase transition during bimanual coordination. *Cereb. Cortex*, **16**, 1338–1348.
- Barr, D.J., Levy, R., Scheepers, C. & Tily, H.J. (2013) Random effects structure for confirmatory hypothesis testing: keep it maximal. *J. Mem. Lang.*, **68**, 225–278.
- Beaulieu, C. (2002) The basis of anisotropic water diffusion in the nervous system – a technical review. *NMR Biomed.*, **15**, 435–455.
- Beets, I.A., Gooijers, J., Boisgontier, M.P., Pauwels, L., Coxon, J.P., Wittenberg, G. & Swinnen, S.P. (2015) Reduced neural differentiation between feedback conditions after bimanual coordination training with and without augmented visual feedback. *Cereb. Cortex*, **25**, 1958–1969.
- Belsley, A.D. (1991). *Conditioning Diagnostics: Collinearity and Weak Data in Regression*. John Wiley & Sons, New York.
- Bennett, I.J., Madden, D.J., Vaidya, C.J., Howard, J.H. Jr & Howard, D.V. (2011) White matter integrity correlates of implicit sequence learning in healthy aging. *Neurobiol. Aging*, **32**, 2317e1–2317e12.
- Berghuis, K.M., De Rond, V., Zijdwind, I., Koch, G., Veldman, M.P. & Hortobagyi, T. (2016) Neuronal mechanisms of motor learning are age dependent. *Neurobiol. Aging*, **46**, 149–159.
- Boisgontier, M.P. & Cheval, B. (2016) The ANOVA to mixed model transition. *Neurosci. Biobehav. R.*, **68**, 1004–1005.
- Boorman, E.D., O'Shea, J., Sebastian, C., Rushworth, M.F. & Johansen-Berg, H. (2007) Individual differences in white-matter microstructure reflect variation in functional connectivity during choice. *Curr. Biol.*, **17**, 1426–1431.
- Brashers-Krug, T., Shadmehr, R. & Bizzi, E. (1996) Consolidation in human motor memory. *Nature*, **382**, 252–255.
- Brown, R.M., Robertson, E.M. & Press, D.Z. (2009) Sequence skill acquisition and off-line learning in normal aging. *PLoS ONE*, **4**, e6683.
- Calamante, F., Tournier, J.D., Jackson, G.D. & Connelly, A. (2010) Track-density imaging (TDI): super-resolution white matter imaging using whole-brain track-density mapping. *NeuroImage*, **53**, 1233–1243.
- Chalavi, S., Zivari, A.H., Pauwels, L., Beets, I.A., Van Ruitenbeek, P., Boisgontier, M.P., Santos Monteiro, T., Maes, C. *et al.* (2016) Anatomy of subcortical structures predicts age-related differences in skill acquisition. *Cereb. Cortex*, **28**, 1–15.
- Cirillo, J., Rogasch, N.C. & Semmler, J.G. (2010) Hemispheric differences in use-dependent corticomotor plasticity in young and old adults. *Exp. Brain Res.*, **205**, 57–68.
- Cirillo, J., Todd, G. & Semmler, J.G. (2011) Corticomotor excitability and plasticity following complex visuomotor training in young and old adults. *Eur. J. Neurosci.*, **34**, 1847–1856.
- Collier, Q., Veraart, J., Jeurissen, B., Den Dekker, A.J. & Sijbers, J. (2015) Iterative reweighted linear least squares for accurate, fast, and robust estimation of diffusion magnetic resonance parameters. *Magn. Reson. Med.*, **73**, 2174–2184.
- Dayan, E. & Cohen, L.G. (2011) Neuroplasticity subserving motor skill learning. *Neuron*, **72**, 443–454.
- Debaere, F., Wenderoth, N., Sunaert, S., Van Hecke, P. & Swinnen, S.P. (2004) Changes in brain activation during the acquisition of a new bimanual coordination task. *Neuropsychologia*, **42**, 855–867.
- Della-Maggiore, V., Scholz, J., Johansen-Berg, H. & Paus, T. (2009) The rate of visuomotor adaptation correlates with cerebellar white-matter microstructure. *Hum. Brain Mapp.*, **30**, 4048–4053.
- Doyon, J., Penhune, V. & Ungerleider, L.G. (2003) Distinct contribution of the cortico-striatal and cortico-cerebellar systems to motor skill learning. *Neuropsychologia*, **41**, 252–262.
- Fields, R.D. (2008) White matter in learning, cognition and psychiatric disorders. *Trends Neurosci.*, **31**, 361–370.
- Fling, B.W., Walsh, C.M., Bangert, A.S., Reuter-Lorenz, P.A., Welsh, R.C. & Seidler, R.D. (2011) Differential callosal contributions to bimanual control in young and older adults. *J. Cognitive Neurosci.*, **23**, 2171–2185.
- Fling, B.W., Benson, B.L. & Seidler, R.D. (2013) Transcallosal sensorimotor fiber tract structure-function relationships. *Hum. Brain Mapp.*, **34**, 384–395.
- Floyer-Lea, A. & Matthews, P.M. (2005) Distinguishable brain activation networks for short- and long-term motor skill learning. *J. Neurophysiol.*, **94**, 512–518.
- Fujiyama, H., Van Soom, J., Rens, G., Gooijers, J., Leunissen, I., Levin, O. & Swinnen, S.P. (2016a) Age-related changes in frontal network structural and functional connectivity in relation to bimanual movement control. *J. Neurosci.*, **36**, 1808–1822.
- Fujiyama, H., Van Soom, J., Rens, G., Cuypers, K., Heise, K.F., Levin, O. & Swinnen, S.P. (2016b) Performing two different actions simultaneously: the critical role of interhemispheric interactions during the preparation of bimanual movement. *Cortex*, **77**, 141–154.
- Giorgio, A., Santelli, L., Tomassini, V., Bosnell, R., Smith, S., De Stefano, N. & Johansen-Berg, H. (2010) Age-related changes in grey and white matter structure throughout adulthood. *NeuroImage*, **51**, 943–951.
- Gooijers, J., Caeyenberghs, K., Sisti, H.M., Geurts, M., Heitger, M.H., Leemans, A. & Swinnen, S.P. (2013) Diffusion tensor imaging metrics of the corpus callosum in relation to bimanual coordination: effect of task complexity and sensory feedback. *Hum. Brain Mapp.*, **34**, 241–252.
- Hair, J.F. Jr, Anderson, R.E., Tatham, R.L. & Black, W.C. (1992). *Multivariate Data Analysis: With Readings*. Macmillan, New York.
- Hardwick, R.M., Rottschy, C., Miall, R.C. & Eickhoff, S.B. (2013) A quantitative meta-analysis and review of motor learning in the human brain. *NeuroImage*, **67**, 283–297.
- Heitger, M.H., Ronsse, R., Dholander, T., Dupont, P., Caeyenberghs, K. & Swinnen, S.P. (2012) Motor learning-induced changes in functional brain connectivity as revealed by means of graph-theoretical network analysis. *NeuroImage*, **61**, 633–650.
- Hoshi, E. & Tanji, J. (2002) Contrasting neuronal activity in the dorsal and ventral premotor areas during preparation to reach. *J. Neurophysiol.*, **87**, 1123–1128.
- Hoshi, E. & Tanji, J. (2004) Functional specialization in dorsal and ventral premotor areas. *Prog. Brain Res.*, **143**, 507–511.
- Howard, D.V. & Howard, J.H. Jr (1992) Adult age differences in the rate of learning serial patterns: evidence from direct and indirect tests. *Psychol. Aging*, **7**, 232–241.
- Jeurissen, B., Leemans, A., Jones, D.K., Tournier, J.D. & Sijbers, J. (2011) Probabilistic fiber tracking using the residual bootstrap with constrained spherical deconvolution. *Hum. Brain Mapp.*, **32**, 461–479.

- Jeurissen, B., Tournier, J.D., Dhollander, T., Connelly, A. & Sijbers, J. (2014) Multi-tissue constrained spherical deconvolution for improved analysis of multi-shell diffusion MRI data. *NeuroImage*, **103**, 411–426.
- Jezzard, P. & Balaban, R.S. (1995) Correction for geometric distortion in echo planar images from B0 field variations. *Magn. Reson. Med.*, **34**, 65–73.
- Jueptner, M., Frith, C.D., Brooks, D.J., Frackowiak, R.S. & Passingham, R.E. (1997) Anatomy of motor learning. II. Subcortical structures and learning by trial and error. *J. Neurophysiol.*, **77**, 1325–1337.
- Kantak, S.S., Stinear, J.W., Buch, E.R. & Cohen, L.G. (2012) Rewiring the brain: potential role of the premotor cortex in motor control, learning, and recovery of function following brain injury. *Neurorehab. Neural Re.*, **26**, 282–292.
- Kantak, S., Jax, S. & Wittenberg, G. (2017) Bimanual coordination: a missing piece of arm rehabilitation after stroke. *Restor. Neurol. Neurosci.*, **35**, 347–364.
- Karni, A., Meyer, G., Rey-Hipolito, C., Jezzard, P., Adams, M.M., Turner, R. & Ungerleider, L.G. (1998) The acquisition of skilled motor performance: fast and slow experience-driven changes in primary motor cortex. *P. Natl. Acad. Sci. USA*, **95**, 861–868.
- Kellner, E., Dhital, B., Kiselev, V.G. & Reiser, M. (2016) Gibbs-ringing artifact removal based on local subvoxel-shifts. *Magn. Reson. Med.*, **76**, 1574–1581.
- King, B.R., Fogel, S.M., Albouy, G. & Doyon, J. (2013) Neural correlates of the age-related changes in motor sequence learning and motor adaptation in older adults. *Front. Hum. Neurosci.*, **7**, 142.
- Leemans, A., Jeurissen, B., Sijbers, J. & Jones, D.K. (2009) ExploreDTI: a graphical toolbox for processing, analyzing, and visualizing diffusion MR data. Proceedings of the 17th scientific meeting, international society for magnetic resonance imaging 2009, Honolulu, USA, p. 3537.
- Maes, C., Gooijers, J., Orban de Xivry, J.J., Swinnen, S.P. & Boisgontier, M.P. (2017) Two hands, one brain, and aging. *Neurosci. Biobehav. R.*, **75**, 234–256.
- Marconi, B., Genovesio, A., Giannetti, S., Molinari, M. & Caminiti, R. (2003) Callosal connections of dorso-lateral premotor cortex. *Eur. J. Neurosci.*, **18**, 775–788.
- Mayka, M.A., Corcos, D.M., Leurgans, S.E. & Vaillancourt, D.E. (2006) Three-dimensional locations and boundaries of motor and premotor cortices as defined by functional brain imaging: a meta-analysis. *NeuroImage*, **31**, 1453–1474.
- Minati, L., Grisoli, M. & Bruzzone, M.G. (2007) MR spectroscopy, functional MRI, and diffusion-tensor imaging in the aging brain: a conceptual review. *J. Geriatr. Psych. Neur.*, **20**, 3–21.
- Nusbaum, A.O., Tang, C.Y., Buchsbaum, M.S., Wei, T.C. & Atlas, S.W. (2001) Regional and global changes in cerebral diffusion with normal aging. *Am. J. Neuroradiol.*, **22**, 136–142.
- Oldfield, R.C. (1971) The assessment and analysis of handedness: the Edinburgh inventory. *Neuropsychologia*, **9**, 97–113.
- O'Shea, J., Sebastian, C., Boorman, E.D., Johansen-Berg, H. & Rushworth, M.F. (2007) Functional specificity of human premotor-motor cortical interactions during action selection. *Eur. J. Neurosci.*, **26**, 2085–2095.
- Pauwels, L., Vancleef, K., Swinnen, S.P. & Beets, I.A. (2015) Challenge to promote change: both young and older adults benefit from contextual interference. *Front. Aging Neurosci.*, **7**, 157.
- Perrot, A. & Bertsch, J. (2007) Role of age in relation between two kinds of abilities and performance in acquisition of new motor skill. *Percept. Motor Skill*, **104**, 91–101.
- Puttemans, V., Wenderoth, N. & Swinnen, S.P. (2005) Changes in brain activation during the acquisition of a multifrequency bimanual coordination task: from the cognitive stage to advanced levels of automaticity. *J. Neurosci.*, **25**, 4270–4278.
- Reinkensmeyer, D.J., Burdet, E., Casadio, M., Krakauer, J.W., Kwakkel, G., Lang, C.E., Swinnen, S.P., Ward, N.S. *et al.* (2016) Computational neurorehabilitation: modeling plasticity and learning to predict recovery. *J. Neuroeng. Rehabil.*, **13**, 42.
- Remy, F., Wenderoth, N., Lipkens, K. & Swinnen, S.P. (2008) Acquisition of a new bimanual coordination pattern modulates the cerebral activations elicited by an intrinsic pattern: an fMRI study. *Cortex*, **44**, 482–493.
- Ren, J., Huang, S., Zhang, J., Zhu, Q., Wilson, A.D., Snapp-Childs, W. & Bingham, G.P. (2015) The 50s cliff: a decline in perceptuo-motor learning, not a deficit in visual motion perception. *PLoS ONE*, **10**, e0121708.
- Ronsse, R., Puttemans, V., Coxon, J.P., Goble, D.J., Wagemans, J., Wenderoth, N. & Swinnen, S.P. (2011) Motor learning with augmented feedback: modality-dependent behavioral and neural consequences. *Cereb. Cortex*, **21**, 1283–1294.
- Ruddy, K.L., Leemans, A. & Carson, R.G. (2017) Transcallosal connectivity of the human cortical motor network. *Brain Struct. Funct.*, **222**, 1243–1252.
- Sadato, N., Yonekura, Y., Waki, A., Yamada, H. & Ishii, Y. (1997) Role of the supplementary motor area and the right premotor cortex in the coordination of bimanual finger movements. *J. Neurosci.*, **17**, 9667–9674.
- Sakamoto, Y., Ishiguro, M. & Kitagawa, G. (1986). *Akaike Information Criterion Statistics*. Dordrecht: Springer.
- Schubotz, R.I. & Von Cramon, D.Y. (2003) Functional-anatomical concepts of human premotor cortex: evidence from fMRI and PET studies. *NeuroImage*, **20**, S120–S131.
- Schulz, R., Zimmerman, M., Timmermann, J.E., Wessel, M.J., Gerloff, C. & Hummel, F.C. (2014) White matter integrity of motor connections related to training gains in healthy aging. *Neurobiol. Aging*, **35**, 1404–1411.
- Schulz, R., Wessel, M.J., Zimmerman, M., Timmermann, J.E., Gerloff, C. & Hummel, F.C. (2015) White matter integrity of specific dentato-thalamo-cortical pathways is associated with learning gains in precise movement timing. *Cereb. Cortex*, **25**, 1707–1714.
- Seidler, R.D., Bernard, J.A., Burutolu, T.B., Fling, B.W., Gordon, M.T., Gwin, J.T., Kwak, Y. & Lipps, D.B. (2010) Motor control and aging: links to age-related brain structural, functional, and biochemical effects. *Neurosci. Biobehav. R.*, **34**, 721–733.
- Serbruyns, L., Gooijers, J., Caeyenberghs, K., Meesen, R.L., Cuypers, K., Sisti, H.M., Leemans, A. & Swinnen, S.P. (2015) Bimanual motor deficits in older adults predicted by diffusion tensor imaging metrics of corpus callosum subregions. *Brain Struct. Funct.*, **220**, 273–290.
- Serrien, D.J. & Brown, P. (2003) The integration of cortical and behavioural dynamics during initial learning of a motor task. *Eur. J. Neurosci.*, **17**, 1098–1104.
- Sisti, H.M., Geurts, M., Clerckx, R., Gooijers, J., Coxon, J.P., Heitger, M.H., Caeyenberghs, K., Beets, I.A.M. *et al.* (2011) Testing multiple coordination constraints with a novel bimanual visuomotor task. *PLoS ONE*, **6**, e23619.
- Sisti, H.M., Geurts, M., Gooijers, J., Heitger, M.H., Caeyenberghs, K., Beets, I.A., Serbruyns, L., Leemans, A. *et al.* (2012) Microstructural organization of corpus callosum projections to prefrontal cortex predicts bimanual motor learning. *Learn. Memory*, **19**, 351–357.
- Smith, S.M., Jenkinson, M., Johansen-Berg, H., Rueckert, D., Nichols, T.E., Mackay, C.E., Watkins, K.E., Ciccarelli, O. *et al.* (2006) Tract-based spatial statistics: voxelwise analysis of multi-subject diffusion data. *NeuroImage*, **31**, 1487–1505.
- Sullivan, E.V. & Pfefferbaum, A. (2006) Diffusion tensor imaging and aging. *Neurosci. Biobehav. R.*, **30**, 749–761.
- Sullivan, E.V. & Pfefferbaum, A. (2007) Neuroradiological characterization of normal adult ageing. *Brit. J. Radiol.*, **80**, S99–S108.
- Sullivan, E.V., Rohlfing, T. & Pfefferbaum, A. (2010) Quantitative fiber tracking of lateral and interhemispheric white matter systems in normal aging: relations to timed performance. *Neurobiol. Aging*, **31**, 464–481.
- Sun, F.T., Miller, L.M., Rao, A.A. & D'Esposito, M. (2007) Functional connectivity of cortical networks involved in bimanual motor sequence learning. *Cereb. Cortex*, **17**, 1227–1234.
- Swinnen, S.P., Verschueren, S.M.P., Bogaerts, H., Dounskaia, N., Lee, T.D., Stelmach, G.E. & Serrien, D.J. (1998) Age-related deficits in motor learning and differences in feedback processing during the production of a bimanual coordination pattern. *Cogn. Neuropsychol.*, **15**, 439–466.
- Tomassini, V., Jbabdi, S., Kincses, Z.T., Bosnell, R., Douaud, G., Pozzilli, C., Matthews, P.M. & Johansen-Berg, H. (2011) Structural and functional bases for individual differences in motor learning. *Hum. Brain Mapp.*, **32**, 494–508.
- Tournier, J.D., Calamante, F. & Connelly, A. (2007) Robust determination of the fibre orientation distribution in diffusion MRI: non-negativity constrained super-resolved spherical deconvolution. *NeuroImage*, **35**, 1459–1472.
- Tournier, J.D., Calamante, F. & Connelly, A. (2010) Improved probabilistic streamlines tractography by 2nd order integration over fibre orientation distributions. Proceedings of the 18th scientific meeting, international society for magnetic resonance imaging 2010, Stockholm, Sweden, p. 1670.
- Tournier, J.D., Mori, S. & Leemans, A. (2011) Diffusion tensor imaging and beyond. *Magn. Reson. Med.*, **65**, 1532–1556.
- Tournier, J.D., Calamante, F. & Connelly, A. (2013) Determination of the appropriate b value and number of gradient directions for high-angular-resolution diffusion-weighted imaging. *NMR Biomed.*, **26**, 1775–1786.
- Tustison, N.J., Avants, B.B., Cook, P.A., Zheng, Y., Egan, A., Yushkevich, P.A. & Gee, J.C. (2010) N4ITK: improved N3 bias correction. *IEEE T. Med. Imaging*, **29**, 1310–1320.
- Van den Berg, F.E., Swinnen, S.P. & Wenderoth, N. (2010) Hemispheric asymmetries of the premotor cortex are task specific as revealed by

- disruptive TMS during bimanual versus unimanual movements. *Cereb. Cortex*, **20**, 2842–2851.
- Vega-Gonzalez, A. & Granat, M.H. (2005) Continuous monitoring of upper-limb activity in a free-living environment. *Arch. Phys. Med. Rehab.*, **86**, 541–548.
- Voelcker-Rehage, C. & Willimczik, K. (2006) Motor plasticity in a juggling task in older adults—a developmental study. *Age Ageing*, **35**, 422–427.
- Voineskos, A.N., Rajji, T.K., Lobaugh, N.J., Miranda, D., Shenton, M.E., Kennedy, J.L., Pollock, B.G. & Mulsant, B.H. (2012) Age-related decline in white matter tract integrity and cognitive performance: a DTI tractography and structural equation modeling study. *Neurobiol. Aging*, **33**, 21–34.
- Wahl, M., Lauterbach-Soon, B., Hattingen, E., Jung, P., Singer, O., Volz, S., Klein, J.C., Steinmetz, H. *et al.* (2007) Human motor corpus callosum: topography, somatotopy, and link between microstructure and function. *J. Neurosci.*, **27**, 12132–12138.
- Wenderoth, N., Debaere, F., Sunaert, S., Van Hecke, P. & Swinnen, S.P. (2004) Parieto-premotor areas mediate directional interference during bimanual movements. *Cereb. Cortex*, **14**, 1153–1163.
- Wilkins, B., Lee, N., Gajawelli, N., Law, M. & Lepore, N. (2015) Fiber estimation and tractography in diffusion MRI: development of simulated brain images and comparison of multi-fiber analysis methods at clinical b-values. *NeuroImage*, **109**, 341–356.
- Wishart, L.R., Lee, T.D., Cunningham, S.J. & Murdoch, J.E. (2002) Age-related differences and the role of augmented visual feedback in learning a bimanual coordination pattern. *Acta Psychol.*, **110**, 247–263.
- Zahr, N.M., Rohlfing, T., Pfefferbaum, A. & Sullivan, E.V. (2009) Problem solving, working memory, and motor correlates of association and commissural fiber bundles in normal aging: a quantitative fiber tracking study. *NeuroImage*, **44**, 1050–1062.
- Zarei, M., Johansen-Berg, H., Smith, S., Ciccarelli, O., Thompson, A.J. & Matthews, P.M. (2006) Functional anatomy of interhemispheric cortical connections in the human brain. *J. Anat.*, **209**, 311–320.
- Zimmerman, M., Nitsch, M., Giroux, P., Gerloff, C., Cohen, L.G. & Hummel, F.C. (2013) Neuroenhancement of the aging brain: restoring skill acquisition in old subjects. *Ann. Neurol.*, **73**, 10–15.